

Stimulated emission of phonons in a ruby fiber

P. A. Fokker, W. D. Koster, J. I. Dijkhuis, and H. W. de Wijn
*Faculty of Physics and Astronomy, and Debye Research Institute, Utrecht University,
 P.O. Box 80000, 3508 TA Utrecht, The Netherlands*

L. Lu, R. S. Meltzer, and W. M. Yen
*Faculty of Physics and Astronomy, University of Georgia, Athens, Georgia 30602
 (Received 10 March 1997)*

Avalanches of resonant phonons generated by stimulated emission within the optically excited $\bar{E}(^2E)$ doublet are observed in a 400- μm thick fiber of single-crystalline ruby. In comparison with bulk ruby, the avalanches develop fully in a shorter time because the phonons are confined to the active medium by reflection from the fiber boundaries. Position-independent rate equations adequately describe the dynamics.
 [S0163-1829(97)05030-3]

Recent experiments on phonon avalanches in optically pumped ruby¹ have shown that the geometry of the crystal and the active zone plays a crucial role in the development of the avalanche. A bulk single crystal with parallel end faces was found to act as a phonon cavity, so that the phonons produced by the avalanche repetitively pass through the active zone and the avalanche is amplified further upon each passage. In the present study, we investigate the phonon avalanche in the restrictive geometry of a thin fiber, which is distinct from a bulk crystal in that the phonons reflecting from the outer wall return to the active zone from many more directions and without significant delay. The magnetic-field split $\bar{E}(^2E)$ doublet of Cr^{3+} again serves as active medium, its upper level E_+ being populated over the larger part of the fiber by selective optical excitation. Stimulated emission of phonons then results from resonant one-phonon processes induced by the spin-lattice interaction to the lower $\bar{E}(^2E)$ level E_- . As in Ref. 1, the growth of the phonon avalanche is observed via the luminescence emanating from E_- . The results differ in two respects from avalanches in bulk ruby. First, the avalanches develop in much shorter times, and, second, no repetitive amplification is observed.

The single-crystalline ruby fiber was grown in Athens, Georgia, by the use of the laser-heated pedestal method.² The starting material had a 1000 at. ppm Cr^{3+} concentration, resulting in about 500 at. ppm for the fiber. The crystalline c axis, defined by a seed crystal of known orientation, was at an angle of $\theta \approx 70^\circ$ with the fiber axis. By controlling the growth rate, the fiber was given a uniform thickness of approximately 400 μm . It was cut to a length of 9 mm, and the end faces were polished to provide optical access.

As for the experiments on phonon avalanches, which were conducted in Utrecht, complete initial inversion of the $\bar{E}(^2E)$ doublet was prepared by selective pulsed optical excitation into its upper level E_+ by means of a pulsed dye laser pumped with an excimer laser. The laser pulses had 10-ns duration and 1-mJ energy at a repetition rate of 10 Hz. The laser beam was focused down to excite a cylinder 300 μm in diameter and coaxial with the fiber axis. The Zeeman splitting of the $\bar{E}(^2E)$ doublet equaled $\delta = 1.56 \text{ cm}^{-1}$ in a

magnetic field $H \approx 4 \text{ T}$ parallel to the fiber. Thermal phonons, which would induce undesired relaxation by Orbach and Raman processes,³ were removed by immersion in superfluid helium at 2 K. Under these conditions the direct spin-lattice relaxation time T_1 is 590 μs .⁴

The avalanches were observed via the associated rise in the E_- population. To measure this rise as a function of the time, the Zeeman-split R_1 luminescence emanating from the excited zone was collected at right angles to the fiber over a length of about 4 mm, and analyzed by a double monochromator followed by standard photon counting and multichannel scaling techniques. The temporal resolution was 0.1 μs .

The data are presented in Fig. 1. For a series of initial inversions, the fraction of the initial population that has completed the transition to E_- is plotted as a function of the time following the laser pulse. We first note that phonon avalanches only develop if the initial inversion exceeds a threshold. Above the threshold, where stimulated emission compensates for the loss, the phonon occupation number grows exponentially, until the inversion becomes depleted and the net gain rapidly decreases. Finally, when the gain no longer compensates for the loss, the avalanche ceases, the phonon occupation number drops to its minute thermal value, and further growth of the E_- population takes place at a rate given by T_1 . In Fig. 1, the succession of the various stages in the development of the avalanche is most clearly discerned for moderate inversions.

The physics underlying the development of an avalanche of phonons resonant with the $\bar{E}(^2E)$ doublet has been considered in substantial detail for the case of narrow pencil of light in a ruby crystal of macroscopic size.^{1,5} In this case, the emitted phonons become off resonant with the $\bar{E}(^2E)$ system after traveling over distances of order 0.5 mm because the level splitting is inhomogeneous and because the preferred direction of travel is noncollinear with the excited zone. High spatial directionality nevertheless results, as the avalanche grows exponentially with the distance. Second, phonons which return to their native place after being reflected by the crystalline faces once again take part in the process of stimulated emission. In the experiments of Ref. 1,

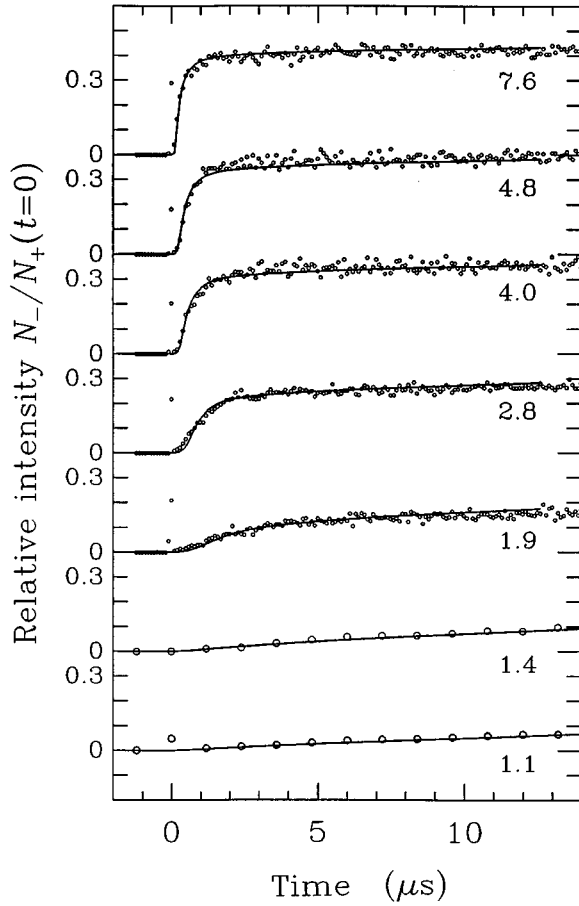


FIG. 1. The growth of the E_- population, as derived from the luminescent intensities, for various initial inversions. The full curves are fits of Eqs. (1)–(3). The labels, proportional to the laser power, denote the initial inversion $N_+(t=0)$ in units 10^{17} cm^{-3} .

the cavity formed by the end faces combined with an active zone of limited size showed up in a recurrent growth of the E_- population with a period equal to the round trip time by way of the end faces.

The geometry of a fiber, by contrast, precludes the formation of a cavity. Reflecting from the outer wall, phonons propagating at a wide spread of angles return to the active zone. This confinement of the phonons to the active medium is quite effective, as both specular and diffusive reflection contribute. Another distinction from a bulk ruby crystal is the time scale on which the phonons return, which is of the order of 50 ns instead of several microseconds in the case of a cavity 10 mm long. Indeed, the avalanche develops straight on to the point of depletion of the inversion on a time scale five times faster than in the bulk under otherwise similar conditions. In the position-dependent formalism of Ref. 1, this corresponds to integration over small distances of travel and the absence of second and further passages.

Under the conditions prevailing in the fiber, therefore, the formalism of Ref. 1 returns to a position-independent set of rate equations for the phonon occupation number p of the resonant modes and the population densities N_+ and N_- of the $\bar{E}(^2E)$ levels. That is,

$$\frac{dp}{dt} = \frac{(p+1)N_+ - pN_-}{\rho\Delta\nu T_1} - \frac{p-p_0}{\tau_1} - \frac{p^2}{\tau_2}, \quad (1)$$

$$\frac{dN_+}{dt} = -\frac{(\varepsilon p+1)N_+ - \varepsilon pN_-}{T_1} - \frac{N_+}{\tau_R}, \quad (2)$$

$$\frac{dN_-}{dt} = \frac{(\varepsilon p+1)N_+ - \varepsilon pN_-}{T_1} - \frac{N_-}{\tau_R}. \quad (3)$$

Here, the terms containing the direct spin-lattice relaxation time T_1 describe the one-phonon processes invoking the avalanche. The quantity ρ denotes the density of phonon states per unit of frequency at the relevant energy, and $\Delta\nu$ is the linewidth of the $\bar{E}(^2E)$ transition. Accordingly, $\rho\Delta\nu$ is the density of resonant phonon modes, which enters Eq. (1) because of the way T_1 is defined. In the Debye approximation, $\rho = 4\pi v^2/v^3$ per acoustic branch, with v the sound velocity. Upon noting that the avalanches are predominantly driven by the two transverse phonon branches ($v = 6.4 \times 10^5 \text{ cm/s}$), we have $\rho = 2.1 \times 10^5 \text{ cm}^{-3} \text{ Hz}^{-1}$ for $\delta = 1.56 \text{ cm}^{-1}$. From frequency-line narrowing (FLN) experiments in bulk ruby,⁶ we find $\Delta\nu = 95 \pm 10 \text{ MHz}$ for $H \approx 4 \text{ T}$ and $\theta \approx 70^\circ$. The parameter ε is the fraction of resonant phonon modes that contribute to the avalanche from geometrical considerations. As pointed out, ε is of order unity for a fiber, as compared to 10^{-2} at most for the highly directional avalanche in bulk ruby. Phonon loss is included by linear and quadratic loss terms with time constants τ_1 and τ_2 , respectively. The linear term, with $p_0 \approx 0.3$ the thermal phonon occupation number, is assumed to include all losses, notably failure to return from the fiber boundaries, but with the exception of anharmonic upconversion. The latter mechanism, represented by a quadratic loss term, is absent at “normal” phonon occupations, but presumably becomes operative at the p reached in the avalanche.^{1,5} The $\bar{E}(^2E)$ population finally returns to the 4A_2 ground state with the radiative decay time $\tau_R \approx 4 \text{ ms}$.

To fit the model to the experimental data in Fig. 1, we first solve the rate equations (1)–(3) numerically to derive $N_-/N_+(0)$ as a function of the time for a series of initial inversions $N_+(0)$ covering the data. Next, these theoretical traces are simultaneously adjusted to all data in Fig. 1 by the use of interpolation and least-squares routines. The adjustable parameters thus are the ratio of the initial inversion over the laser power $N_+(0)/P$, the fraction ε , and the time constants τ_1 and τ_2 . The initial phonon occupation number $p(0)$ was set equal to the thermal value p_0 , where we note that changing $p(0)$ by 50% only insignificantly affects the fitted parameters. The results are $N_+(0)/P = (6.7 \pm 0.7) \times 10^{18} \text{ cm}^{-3}/\text{mJ}$, $\varepsilon = 0.8 \pm 0.3$, $\tau_1 = 68 \pm 7 \text{ ns}$, and $\tau_2 = 45 \pm 8 \mu\text{s}$. The time traces recalculated by inserting the fitted parameters into Eqs. (1)–(3) are entered in Fig. 1 as the full curves, and seen to track the data adequately. The fitting also yielded that p rises to a maximum of 2×10^3 at the highest laser power, the maximum being reached at 200 ns after the inverting laser pulse.

Substantial confirmation for the use of the position-independent equations (1)–(3) is gained from the fitted parameter values. The result for ε indeed is in conformity with the anticipated wide spread in travel directions. The fitted value for $N_+(0)/P$ is quite reasonable in view of the size of the focus and the absorption of laser light by 500 at. ppm ruby. Because a small orientational spread of the c axis would result in a substantially larger $\Delta\nu$,⁶ this also indicates

that the fiber is of a good crystalline quality. The linear phonon lifetime τ_1 found compares with the round trip time for ballistic travel to the fiber boundary in combination with moderate surface reflectivity. Averaging over all directions and positions, we have

$$\tau_1 \sim -\frac{\pi d}{2v \ln R}, \quad (4)$$

with R the reflection coefficient, either specular or diffusive, d the diameter of the fiber, and v the phonon velocity. Within the uncertainties, this yields $R=0.3\pm 0.1$ to correspond with the fitted τ_1 .

In summary, stimulated emission of resonant phonons has

been observed in a thin fiber of dilute ruby. The geometry is such that the generated phonons are essentially confined to an extended active zone, which spoils the formation of an acoustical cavity and the inherent high directionality observed in bulk ruby, but at the same time makes stimulated emission exceedingly efficient.

The work was supported by the Netherlands Foundation Fundamenteel Onderzoek der Materie (FOM), the Nederlandse Organisatie voor Wetenschappelijk Onderzoek (NWO), the U.S. National Science Foundation (Grant No. DMR 9015468), and NATO (Collaborative Research Grant No. 890931).

¹P. A. Fokker, J. I. Dijkhuis, and H. W. de Wijn, *Phys. Rev. B* **55**, 2925 (1997).

²B. M. Tissue, Lizhu Lu, and W. M. Yen, *J. Lumin.* **45**, 20 (1990).

³S. Geschwind, R. J. Collins, and A. L. Schawlow, *Phys. Rev. Lett.* **3**, 545 (1959); S. Geschwind, G. E. Devlin, R. L. Cohen, and S. R. Chinn, *Phys. Rev.* **137**, A1087 (1965).

⁴J. I. Dijkhuis, K. Huibregtse, and H. W. de Wijn, *Phys. Rev. B* **20**, 1835 (1979).

⁵J. G. M. van Miltenburg, G. J. Jongerden, J. I. Dijkhuis, and H.

W. de Wijn, in *Phonon Scattering in Condensed Matter*, edited by W. Eisenmenger, K. Laßmann, and S. Döttinger (Springer-Verlag, Berlin, 1984), p. 130.

⁶P. A. Fokker, R. J. E. Jaspers, J. I. Dijkhuis, and H. W. de Wijn, (unpublished). The FLN value for $H\approx 4$ T and $\theta\approx 70^\circ$ is larger than the EPR value for $H\approx 1$ T and $\theta\approx 0^\circ$ (Ref. 3), but smaller than the EPR value for $H\approx 6$ T and $\theta\approx 90^\circ$ [Takao Muramoto, *J. Phys. Soc. Jpn.* **35**, 921 (1973)].